Supplementary Information

Photocatalytic and Photoelectrochemical Degradation of Organic Compounds with All-Inorganic Metal Halide Perovskite Quantum Dots

Drialys Cardenas-Morcoso, [†] *Andrés F. Gualdrón-Reyes,* [†, ‡, §] *Ana Beatriz Ferreira-Vitoreti,* [†, □, ǂ] *Miguel García-Tecedor,* [†] *Seog Joon Yoon,* [†] *Mauricio Solis de la Fuente,* [‖] *Iván Mora-Seró,* *[†] *Sixto Gimenez* *[†]

[†] Institute of Advanced Materials (INAM), Universitat Jaume I, 12071 Castelló, Spain

[‡] Centro de Investigaciones en Catálisis (CICAT), Universidad Industrial de Santander, Sede UIS Guatiguará, Piedecuesta, Santander, Colombia. C.P. 681011.

[§] Centro de Investigación Científica y Tecnológica en Materiales y Nanociencias (CMN), Universidad Industrial de Santander, Piedecuesta, Santander, Colombia. C.P. 681011.

[□] Department of Natural Science, Federal University of São João del-Rei, 36301-160 São João del-Rei, Brazil

[ǂ] CAPES Foundation, Ministry of Education of Brazil, Brasília, 70040-020, Brazil

[‖] Lawrence Berkeley National Laboratory, Energy Technologies Area, 1 Cyclotron Road, Berkeley, California 94720, United States of America

[*]**Email:** sero@uji.es, sjulia@uji.es

Experimental methods

Materials and Reagents: All chemicals used for all synthesis were purchased from Sigma-Aldrich, unless otherwise specified. Cesium carbonate (Cs_2CO_3, 99.9 %), lead iodide (PbI_2, ABCR, 99.999 %), lead bromide ($PbBr_2$, TCI, 99.99 %), tin iodide (SnI_2, 99.99 %), oleic acid (OA; technical grade, 90 %), oleylamine (OLA; primary amine, 98 %), trioctylphosphine (TOP; technical grade, 90 %), 1-octadecene (ODE; technical grade, 90 %) and hexane (CHROMASOLV, 95 %), anhydrous methyl acetate (MeOAC, 99,5 %), anhydrous octane (99 %), lead nitrate ($Pb(NO_3)_2$, 99.99 %), acetone (Panreac, 99.5 %) and ethanol (Panreac, 96 %).

Synthesis of $CsPbX_3$ (X = Br, I) and $CsPbBr_{1.5}I_{1.5}$ QDs: The synthesis of $CsPbX_3$ and $CsPbBr_{1.5}I_{1.5}$ QDs was performed following the procedure described by Kovalenko and coworkers.[1] First, Cs-oleate solution was prepared dissolving 0.61 g of Cs_2CO_3, 1.88 mL of OA and 30 mL of ODE in a 50 mL-three neck flask at 120°C, under vacuum for 1 h, under stirring. Then, the flask was purged with N_2 and heated at 150°C, until the solution became clear. The Cs-oleate solution was cooled and stored under N_2 to carry out the QDs preparation.

To prepare $CsPbX_3$ (X = Br, I) and $CsPbBr_{1.5}I_{1.5}$ QDs, the corresponding halide precursor (0.69 g of $PbBr_2$ or 0.87 g of PbI_2) or the mixture and 50 mL of ODE were loaded into a 100 mL-three neck flask and degassed for 1 h at 120°C, under stirring. Then, the flask was purged with N_2, and OA and subsequently OLA (5 mL of each one) were injected at 120°C. The reaction flask was degassed for 1 min until the total dissolution of halide precursor was completed. The flask was again purged with N_2 and quickly heated to 170°C. Once the reaction temperature was reached, 4 mL of preheated Cs-oleate was rapidly added to the reaction flask and after 5 s, the reaction was quenched by cooling in an ice bath.

Synthesis of $CsPb_{0.4}Sn_{0.6}I_3$ QDs: $CsPb_{0.4}Sn_{0.6}I_3$ QDs were synthetized according with the reported method of Shen and coworkers.[2] Briefly, 0.74 g SnI_2 and 0.35 g PbI_2 were mixed in 2.5 mL TOP, to prepare the SnI_2-PbI_2 precursor solution. The solution was heated at 90°C for 5 h. On the other hand, 0.12 g of Cs_2CO_3, 0.4 mL of OA and 0.4 mL OLA were added to a 12 mL of ODE, in a 50 mL-three neck flask. The reaction mixture was degassed at 100°C for 3 h under stirring, and purged with N_2 at 120°C, to achieve a clear solution. The reaction temperature was increased to 170°C, followed by

the fast injection of SnI_2-PbI_2 precursor solution. The reaction quenching was carried out by cooling in ice bath for 5 s. The as-synthetized $CsPbBr_3$, $CsPbI_3$, $CsPbBr_{1.5}I_{1.5}$ and $CsPb_{0.4}Sn_{0.6}I_3$ QDs were centrifuged at 4700 rpm for 5 min to separate the aggregated nanoparticles. After centrifugation, the supernatant was discarded and the QDs pellets were redispersed in hexane to prepare long-term stable colloidal solutions.

Purification of $CsPbBr_3$ QD: To isolate the $CsPbBr_3$ QDs, two-step purification was achieved. For the first step, 70 mL of MeOAc were added to 32 mL of colloidal QDs solution and then centrifuged at 4700 rpm for 10 min. After discarding the supernatant, the QDs solid was dispersed in 8 mL of hexane. In the second purification step, 10 mL of MeAOc was loaded to the dispersion of QDs, and then centrifuged at 4700 rpm for 5 min. After discarding the supernatant, the purified QDs were dispersed in 10 mL of hexane and stored at low temperature at least for 48 h, to decant residual products as Cs and Pb oleates. The colloidal QDs solution was dried with a N_2 flow and the final QDs precipitate was concentrated at 50 $mgmL^{-1}$ with hexane.

Preparation of $CsPbBr_3$ QD films: Prior to film preparation FTO substrates (Pilkington, TEC-15) were rinsed with soap/Milli-Q water, acetone and ethanol, each one for 15 min. After drying the substrates under air flow, the conducting surface was cleaned under UV-O_3 for 15 min. Then, TiO_2 compact layer was deposited on FTO by spin-casting 80 μL of a Ti-alkoxide solution (ShareChem, SC-BT060) at a spin rate of 4000 rpm for 30 s. The as-deposited TiO_2 layer was dried at 150°C for 10 min, and then annealed at 500°C for 30 min. The purified $CsPbBr_3$ QDs solution in octane was deposited by spin-coating on TiO_2 compact layer at 1000 rpm for 20 s. The as-prepared films were dipped into a solution composed by 10 mg mL^{-1} of $Pb(NO_3)_2$ in MeOAc and rinsed with neat MeOAc. The procedure to prepare the $Pb(NO_3)_2$/MeOAc solution is reported elsewhere.[3] The QDs deposition and dipping into $Pb(NO_3)_2$/MeOAc solution was repeated 4 times.

Structural and optical characterization of perovskite QDs: XRD diffraction data was collected on a Rigaku Miniflex 600, (Rigaku corporation, Tokyo, Japan) with copper K_α radiation (λ = 1.5418 Å) at a scan speed of $3°\cdot min^{-1}$. Transmission electron microscopy (TEM) was performed in a JEM-2100 JEOL transmission electron microscope operating at 100 kV. The absorbance of the colloidal QDs solutions was measured on a Varian Cary 300 Bio spectrophotometer. Photoluminescence (PL)

measurements were done through home-built optical setup with 405 nm continuous (CW) laser (10 mW/cm^2, Thorlabs) as excitation source and charged coupled device (CCD) camera (Andor Monochromator system, DV420A-OE) as detector in visible region. To remove scattered light from the excitation source, 435 nm long pass filter was applied in front of the CCD detector. Ultraviolet Photoelectron Spectroscopy (UPS) was measured in halide perovskite quantum dots (1mg/ml) deposited on corning glass substrates by spin coating (1000rpm). K-Alpha Plus XPS/UPS equipment was used, He I as source gun, analyzer mode pass energy 2.0 eV and energy step size 0.050 eV.

CV measurements of perovskite QDs dispersions: CV measurements were performed on a three-electrode cell and using an Autolab Potentiostat/Galvanostat. A non-aqueous $Ag/AgNO_3$ electrode (ALS, Japan), a Platinum electrode (CHI Instruments, USA, 2 mm of diameter) and a Platinum wire was used as reference, working and counter electrode, respectively. A 100 mM tetrabutylammonium hexafluorophosphate (Bu_4NPF_6; Signa-Aldrich) solution in dichloromethane (DCM; anhydrous, Sigma-Aldrich) was used as supporting electrolyte.[4] The net concentration of QDs was kept as 4 mg mL^{-1} in all the experiments, in a total volume of 10 ml. Before each measurement, the Pt working electrode was polished with 0.3 µm alumina paste, rinsed with deionized water and finally dried with compressed air. All the glassware and solid reactants were dried at 80 ºC for three hours before use. To calibrate the system to the Normal Hydrogen Electrode (NHE) scale, the Ferrocene/Ferrocenium (Fc/Fc^+) couple was used as internal standard,[5] by adding 1.9 mM of ferrocene after the electrochemical tests (see below in **Figure S1**).

Steady-state/time resolved photoluminescence measurements: Steady-state photoluminescence measurements were carried out to validate the band alignment as determined by CV. In all the experiments, a concentration of 0.04 mg/mL of QDs dispersed in hexane was used. Prior to measurements, we monitored the emission change with time after adding pure solvent in order to characterize the dilution effect when mixing two solutions. When checking type-II alignment, in order to differentiate between fast (emission quenching, in few seconds) and slow (halide exchange) processes, continuous spectra were recorded. Time-resolved photoluminescence (TRPL) was measured through photoluminescence spectrophotometer (Fluorolog 3-11, Horiba). 405 nm pulsed laser (1 MHz frequency, NanoLED-405L, <100 ps of pulse width) was

used to excite QDs. All measurements for the TRPL were performed under inert environment with N_2 purged solution to prevent extra excitation quenching.

Photocatalytic degradation of MBT: The photodegradation of MBT was monitored through the optical absorbance at 320 nm, which is the characteristic band for this compound,[6] using a Cary 300 Bio spectrophotometer. The working solution consisted of a mix of 0.08 mg mL^{-1} QDs and 0.03 mM MBT in hexane. This solution was placed inside a quartz cuvette and irradiated at 100 mW cm^{-2} with an Oriel 300 W Xenon lamp. 1 ml aliquots of this solution were extracted every 10 min to monitor the evolution of the absorbance at 320 nm. Electrospray Mass Spectra (ESI-MS) were obtained with a QTOF Premier instrument with an orthogonal Z-spray-electrospray interface (Waters, Manchester, UK). The drying and cone gas was nitrogen set to flow rates of 300 and 30 L/h, respectively. A capillary voltage of 3.5 kV or 2.5 kV was used in the positive ESI(+) and negative ESI(-) scan mode, respectively. The cone voltage was adjusted in both ESI(+) or ESI(-) scan modes to a low value (typically U_c = 10 V) to control the extent of fragmentation in the source region. Sample solutions dissolved in methanol were introduced through a fused-silica capillary to the ESI source via syringe pump at a flow rate of 10 μL/min.

Photoelectrochemical (PEC) measurements in QDs films: cyclic voltammetry, linear sweep voltammetry and chronoamperometric measurements were performed on a three-electrode cell and using an Autolab Potentiostat/Galvanostat were a non-aqueous $Ag/AgNO_3$ electrode (ALS, Japan) and a Platinum wire was used as reference and counter electrode, respectively. A $CsPbBr_3/TiO_2/FTO$ electrode was used as the working electrode. A 0.1 M Bu_4NPF_6; solution in DCM was used as supporting electrolyte. The formal potential of the $Ag/AgNO_3$ electrode was estimated using the Fc/Fc^+ couple as standard. Single Frequency Impedance Spectroscopy measurements (100 Hz) were performed for the determination of the space charge capacitance of the electrodes, by Mott-Schottky analysis through the relation: $C_{SC}^{-2} = \frac{2}{q\varepsilon\varepsilon_0 N_D}\left(V + V_{fb} - \frac{k_B T}{q}\right)$, where q is the elemental charge, ε is the relative dielectric constant of the $CsPbBr_3$ QDs (4.96 [1]), ε_0 the vacuum permittivity, N_D is the donor density, V is the applied potential and $k_B T$ the Boltzmann constant times the temperature.

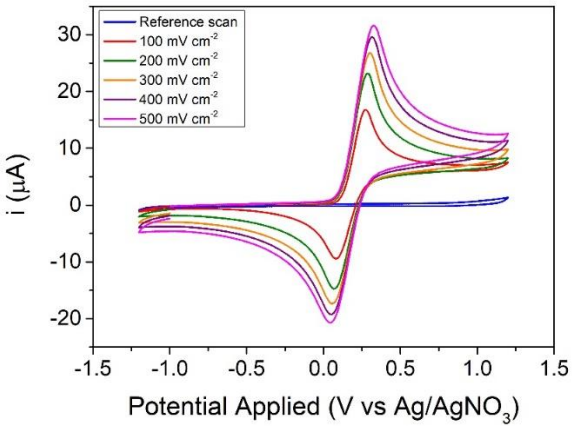

Figure S1. CV measurement at different scan rate of the $Fc^{+/0}$ couple with which the system was calibrated. The molar concentration of ferrocene was 1.9 mM. Reference scan was performed in 0.1 M Bu_4NPF_6 in dichloromethane electrolyte.

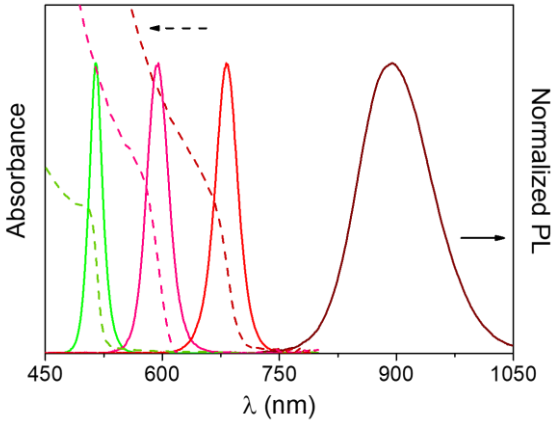

Figure S2. Absorbance (dashed lines) and PL spectra (straight lines) of $CsPbBr_3$ (green), $CsPb(Br_{0.5}I_{0.5})_3$ (pink), $CsPbI_3$ (red) and $CsPb_{0.4}Sn_{0.6}I_3$ (dark red) QDs.

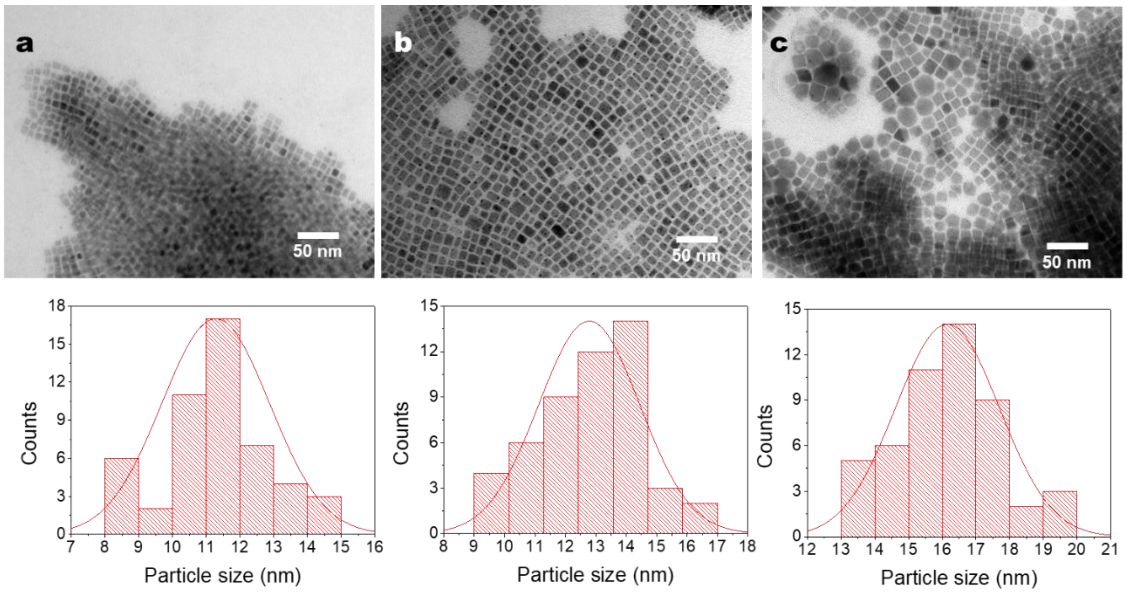

Figure S3. TEM micrographies and histograms with the particles size distribution of the $CsPbBr_3$, $CsPb(Br_{0.5}I_{0.5})_3$ and $CsPbI_3$.

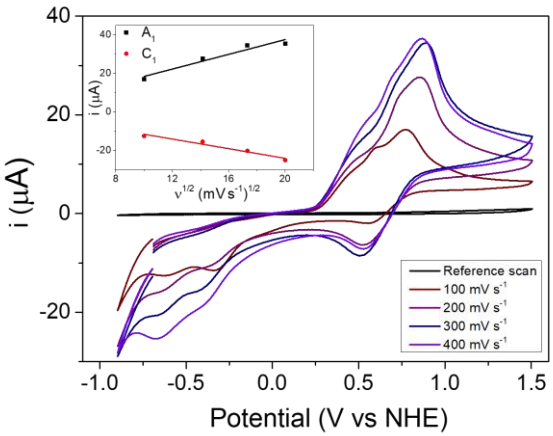

Figure S4. CV in a $CsPb_{0.4}Sn_{0.6}I_3$ QDs dispersion at different scan rates. As inset, linear fitting of A_1 and C_1 peak currents vs $\nu^{1/2}$, confirming the diffusion-controlled process.

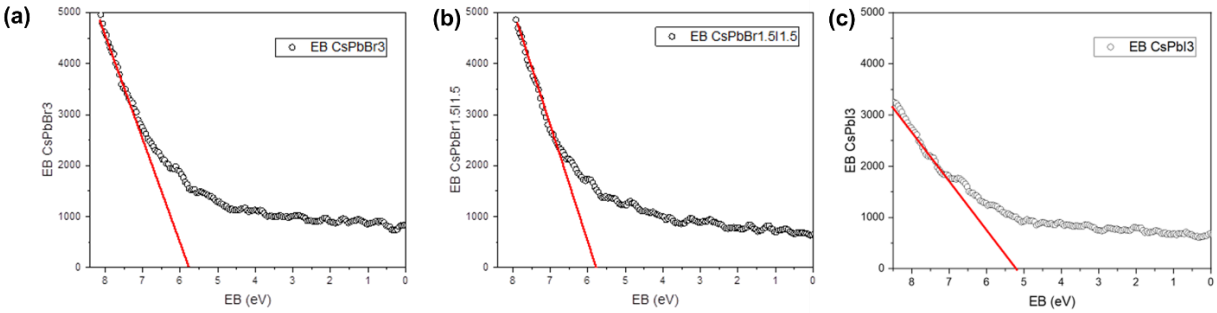

Figure S5. UPS for VB position determination.

Discussion about PL measurements to validate band positions

As shown in **Figure S6a**, type I alignment allows charge transfer of both carriers from the material with wider band gap (donor) to that with narrower band gap (acceptor), which should be reflected on increased PL emission of the acceptor and decreased emission of the donor. Conversely, type II alignment allows asymmetrical charge transfer between both systems and should result in the quenching of the PL emission of both components.[7-8] **Figures S6b-f** illustrate the change in emission properties of the different studied QDs, upon addition of a second chromophore. In **Figure S6b**, the emission from $CsPbI_3$ QDs was drastically decreased about 83% of initial emission intensity. However, PL from $CsPb_{0.4}Sn_{0.6}I_3$ remains unaltered after $CsPbI_3$ addition (**Figure S6b, inset**), indicating type I alignment if dilution effect is considered (discussed below). In contrast, as shown in **Figure S6c-d** and **Figure S6e-f**, emissions from both constituents were quenched when another QDs solution was added indicating type II alignment. It must be highlighted that in all cases, the PL measurements for the determination of the type-II alignment were carried out in a short term (few seconds) after addition of second QDs solution to clearly differentiate from long term process (few minutes), halide exchange between two different halide perovskite QDs (**Figure S7**).[9] As described earlier, the quenching of the emissions from both components reflects type-II alignment between $CsPb_{0.4}Sn_{0.6}I_3/CsPbBr_3$, and between $CsPbBr_3/CsPbI_3$.

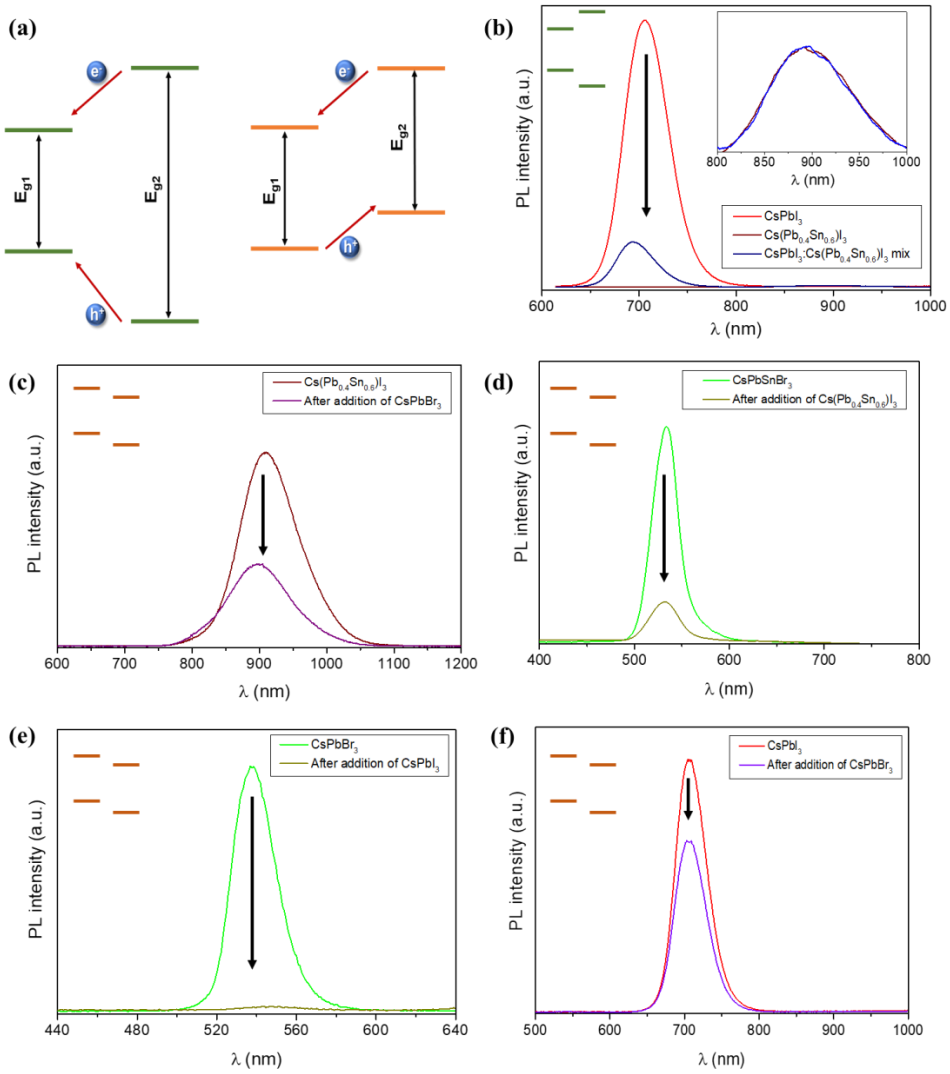

Figure S6. (a) Scheme indicating type I (left) and type II (right) interactions between two different chromophores. PL measurements showing the interaction between the studied perovskite QDs: **(b)** 'Type-I' interaction between $CsPbI_3/Cs(Pb_{0.4}Sn_{0.6})I_3$; **(c)-(d)** 'Type-II' interaction between $CsPbBr_3/Cs(Pb_{0.4}Sn_{0.6})I_3$. **(e)-(f)** 'Type-II' interaction between $CsPbBr_3/Cs(Pb_{0.4}Sn_{0.6})I_3$ and $CsPbBr_3/CsPbI_3$. In **(b)-(f)**, the relative band alignment for the corresponding system is schematically indicated.

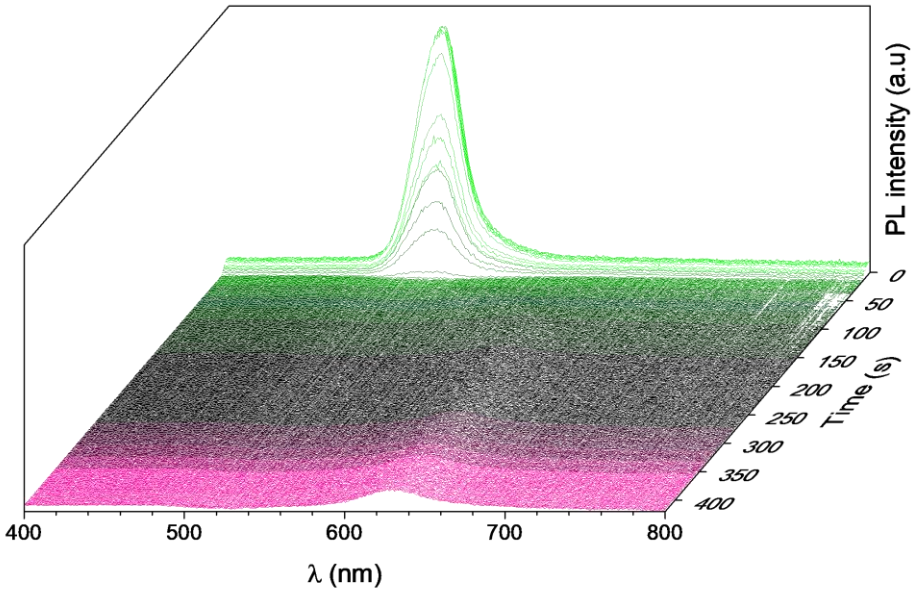

Figure S7. Kinetic PL measurement showing emission quenching and halide mixing ($CsPbBr_3$/$CsPbI_3$) in their respective time scales.

Dilution effect

To consider dilution effect, in an initial 0.8 mg mL^{-1} concentration of the $CsPbBr_3$ QDs dispersion, hexane was added to a final concentration of 0.4 mg mL^{-1}. By simply considering the dilution effect, the emission intensity should decrease less than 10% as shown in **Figure S8**.

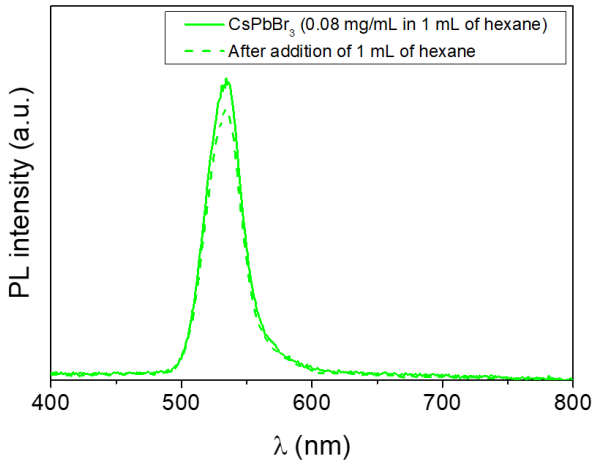

Figure S8. Effect of dissolution on PL emission when adding hexane.

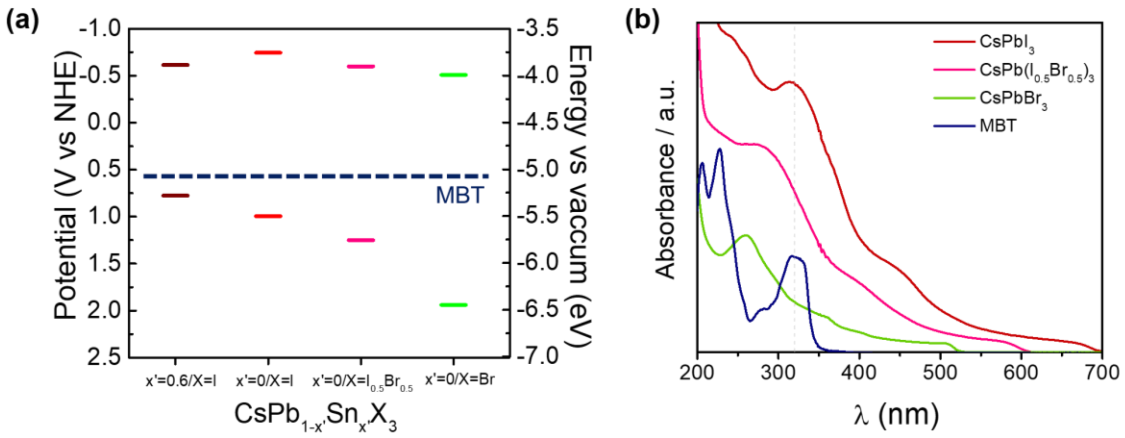

Figure S9. (a) Energy diagram obtained through CV of the QDs and the averaged redox potential reported for MBT. **(b)** Absorbance spectra of the QDs and the MBT, showing the optimal behavior of $CsPbBr_3$ for testing the photocatalytic activity through optical measurements.

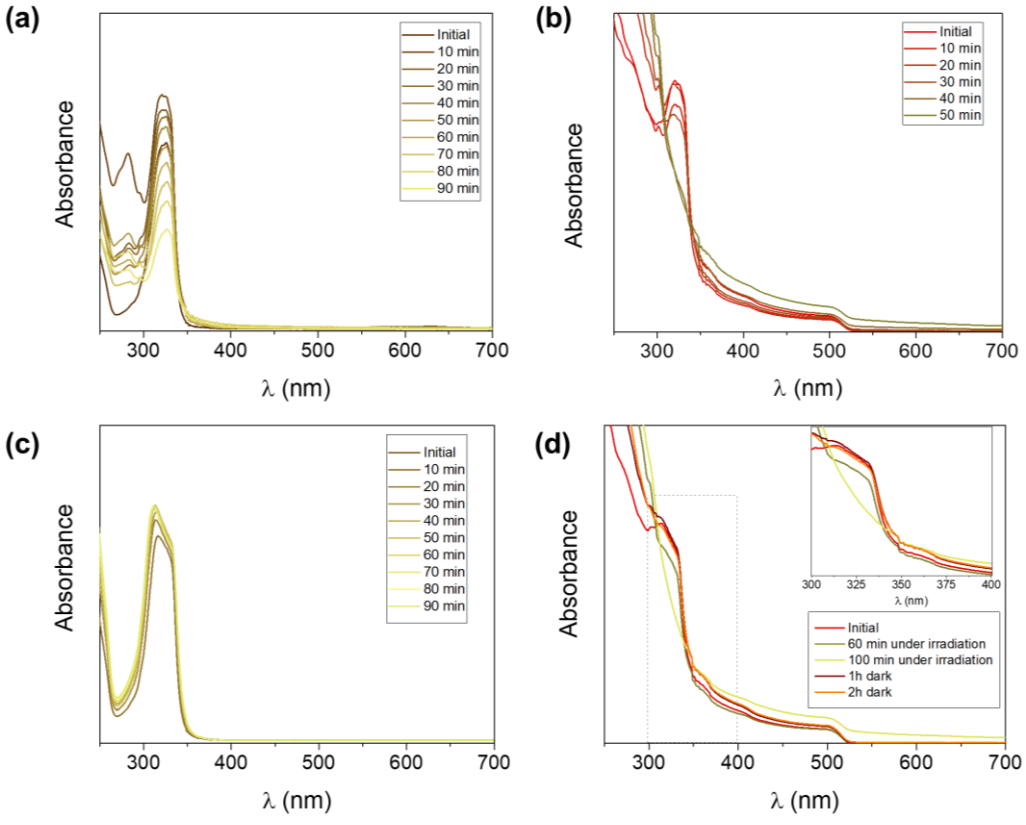

Figure S10. Absorbance spectra of MBT photodegradation under 100 mW cm^{-2} irradiation **(a)** MBT in hexane, **(b)** MBT and $CsPbBr_3$ QDs in hexane, **(c)** MBT in hexane and UV filter, **(d)** Control measurements with MBT and $CsPbBr_3$ QDs in hexane kept in dark condition.

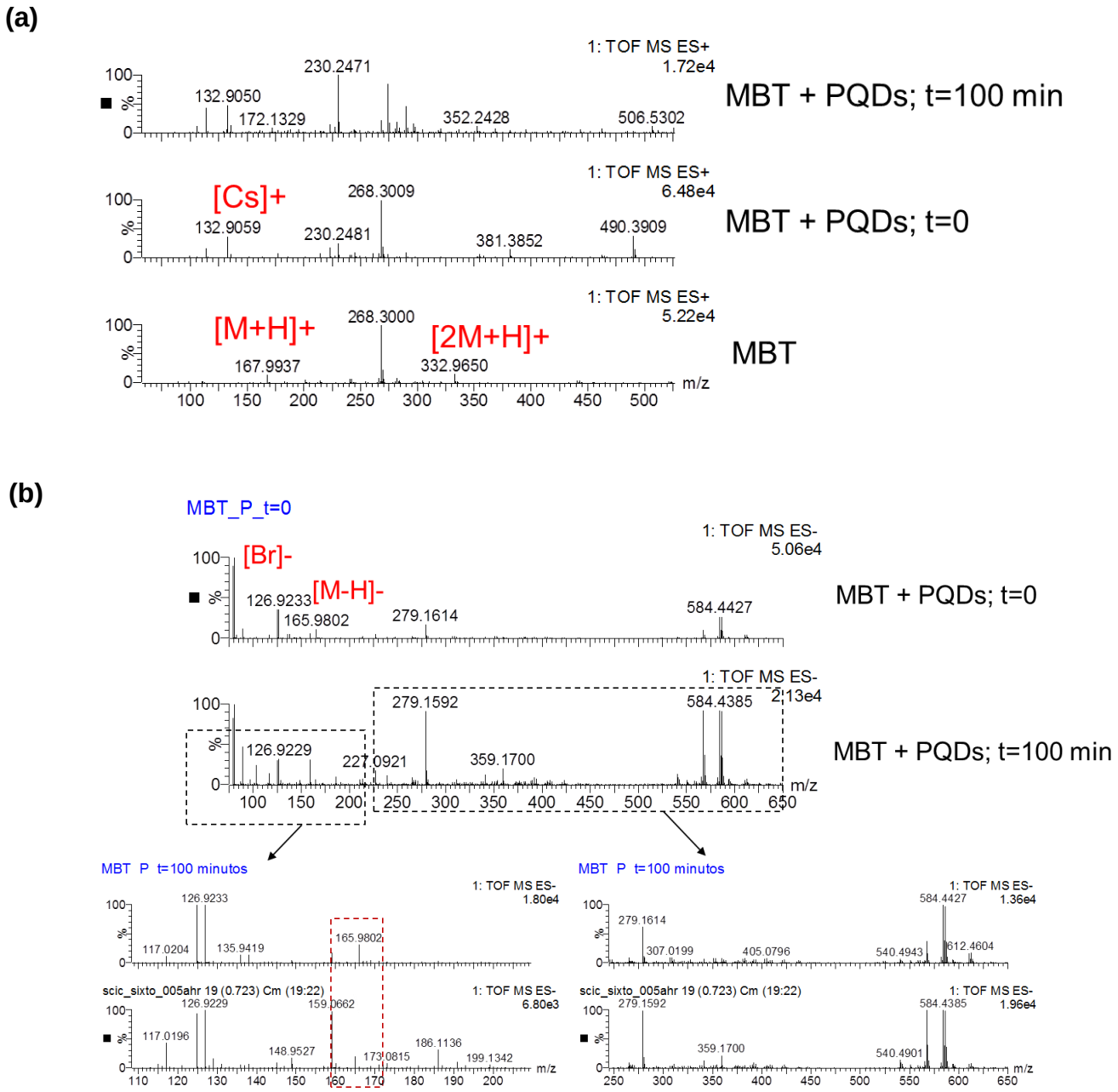

Figure S11. ESI-MS performed in a control sample of MBT in hexane, and then with the $CsPbBr_3$ QDs incorporated before (t=0) and after (t=100 min) 100 mW cm^{-2} irradiation using a UV filter. **(a)** $ESI^{(+)}$, **(b)** $ESI^{(-)}$

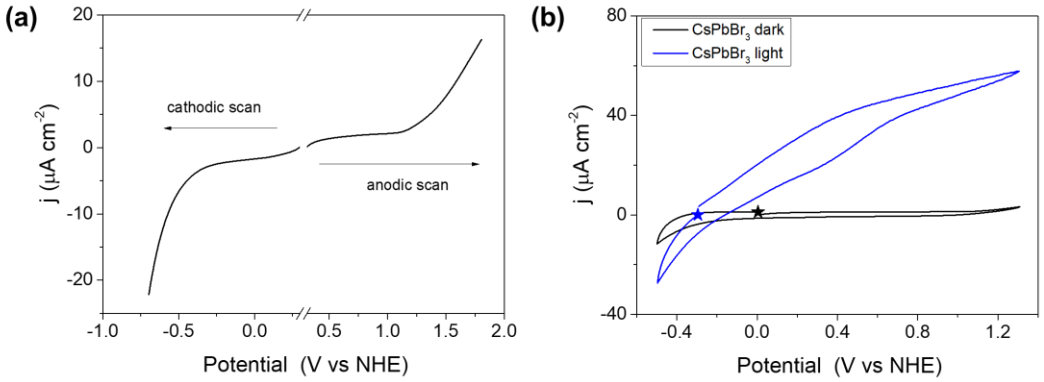

Figure S12. (a) Linear sweep voltammetry performed separately in anodic and cathodic directions in $CsPbBr_3$/c-TiO_2/FTO film in dark, to determine the optimal voltage window for PEC characterization preventing degradation of the $CsPbBr_3$ QDs. **(b)** Cyclic voltammetry in $CsPbBr_3$/c-TiO_2/FTO film in dark and under 1 sun illumination. The stars symbols mark the starting value of each scan, which is the OCP value.

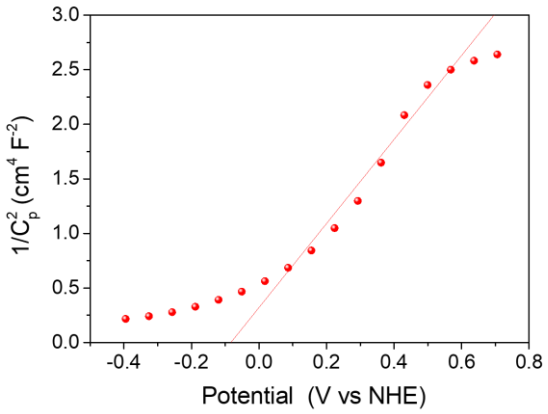

Figure S13. Mott-Schottky plot on $CsPbBr_3$/c-TiO_2/FTO film. (Performed at single frecuency; 500 Hz)

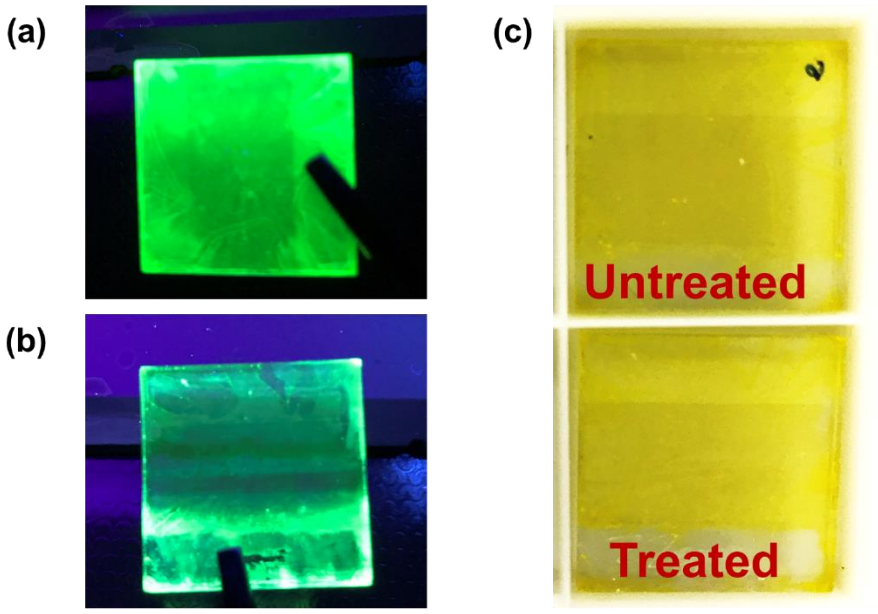

Figure S14. (a) Digital picture of the $CsPbBr_3$/c-TiO_2/FTO film under UV light before and (b) after several PEC measurements (linear and cyclic voltammetry and chronoamperometry in dark and under illumination conditions). (c) Comparison between and untreated sample and a treated one.

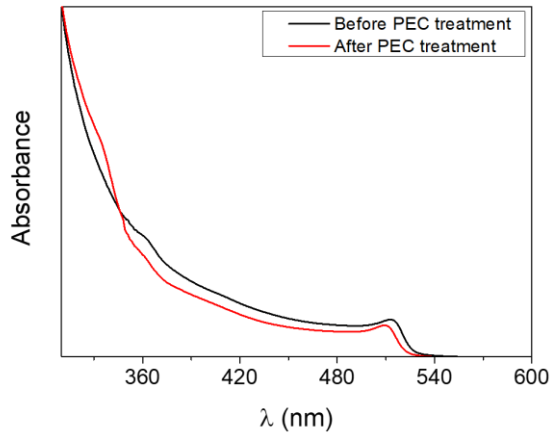

Figure S15. Absorbance spectra of the $CsPbBr_3$/c-TiO_2/FTO film before and after PEC measurements.

Table S1. Summary of the survey of the different salt support/solvent combinations tested to ascertain the stability of the QDs solutions during the photocatalytic/photoelectrochemical tests. Unstable combinations (☹) and stable combination (☺) are indicated.

Solvent / Support salt	Toluene/DCM	Hexane/DCM
TBA-TFB	☹	☹
TBA-P	☹	☹
TBA-DHP	☹	☹
TBA-HFP	☹	☺

TBA-TFB= Tetrabutylammonium tetrafluoroborate
TBA-P= Tetrabutylammonium perchlorate
TBA-DHP= Tetrabutylammonium dihydrogenphosphate
TBA-HFP= Tetrabutylammonium hexafluorophosphate

Table S2. Band structure parameters obtained from CV measurements of the investigated QDs.

QDs	Optical E_g (eV)	VB (V vs NHE)	CB (V vs NHE)	Electrochemical E_g (eV)	VB from UPS (V vs NHE)
$CsPbI_3$	1.7	0.995	-0.745	1.74	0.68
$CsPb_{1-x}Sn_xI_3$	1.4	0.775	-0.615	1.39	-
$CsPb(I_{0.5}Br_{0.5})_3$	1.77	1.25	-0.6	1.84	1.28
$CsPbBr_3$	2.4	2.145	-0.315	2.46	1.3

Table S3. Correlation between the band alignment estimated from electrochemical measurements (cyclic voltammetry) and optical measurements (photoluminescence).

Interacting materials	Alignment from CV	Alignment from PL
$CsPbI_3$ and $Cs(Pb_{0.4}Sn_{0.6})I_3$	I	I
$CsPbI_3$ and $CsPb(I_{0.5}Br_{0.5})_3$	II	N/A
$CsPbI_3$ and $CsPbBr_3$	II	II

$Cs(Pb_{0.4}Sn_{0.6})I_3$ and $CsPb(I_{0.5}Br_{0.5})_3$	I	N/A
$Cs(Pb_{0.4}Sn_{0.6})I_3$ and $CsPbBr_3$	II	II
$CsPb(I_{0.5}Br_{0.5})_3$ and $CsPbBr_3$	II	N/A

Table S4. Results of triexponential fitting ($y = A_1e^{-x/\tau_1} + A_2e^{-x/\tau_2} + A_3e^{-x/\tau_3}$) of the time-resolved PL from $CsPbBr_3$ PQD with MBT solution with subject to illumination time. A_i, τ_i, $<\tau>$, χ^2 represent amplitude, lifetime, average lifetime ($<\tau> = \frac{\Sigma A_i\tau_i^2}{\Sigma A_i\tau_i}$), chi square value, respectively.

Irradiation time	**A_1**	**τ_1 (ns)**	**A_2**	**τ_2 (ns)**	**A_3**	**τ_3 (ns)**	**$<\tau>$ (ns)**	**χ^2**
0 min	0.125	2.03	0.427	8.00	0.448	31.2	26.3	1.15
5 min	0.110	1.34	0.467	5.90	0.423	23.2	19.2	1.01
15 min	0.163	1.27	0.543	5.93	0.294	21.2	15.6	1.09
45 min	0.569	0.861	0.341	4.13	0.0901	19.4	11.0	1.55
90 min	0.661	0.785	0.312	3.37	0.0268	30.6	12.1	1.15

References

(1) Protesescu, L.; Yakunin, S.; Bodnarchuk, M. I.; Krieg, F.; Caputo, R.; Hendon, C. H.; Yang, R. X.; Walsh, A.; Kovalenko, M. V. Nanocrystals of Cesium Lead Halide Perovskites ($CsPbX_3$, X = Cl, Br, and I): Novel Optoelectronic Materials Showing Bright Emission with Wide Color Gamut. *Nano Letters* **2015,** *15* , 3692-3696.

(2) Liu, F.; Ding, C.; Zhang, Y.; Ripolles, T. S.; Kamisaka, T.; Toyoda, T.; Hayase, S.; Minemoto, T.; Yoshino, K.; Dai, S.; Yanagida, M.; Noguchi, H.; Shen, Q. Colloidal Synthesis of Air-Stable Alloyed $CsSn_{1-x}Pb_xI_3$ Perovskite Nanocrystals for Use in Solar Cells. *Journal of the American Chemical Society* **2017,** *139* , 16708-16719.

(3) Sanehira, E. M.; Marshall, A. R.; Christians, J. A.; Harvey, S. P.; Ciesielski, P. N.; Wheeler, L. M.; Schulz, P.; Lin, L. Y.; Beard, M. C.; Luther, J. M. Enhanced Mobility $CsPbI_3$ Quantum Dot Arrays For Record-Efficiency, High-Voltage Photovoltaic Cells. *Science Advances* **2017,** *3*.

(4) Samu, G. F.; Scheidt, R. A.; Kamat, P. V.; Janáky, C. Electrochemistry and Spectroelectrochemistry of Lead Halide Perovskite Films: Materials Science Aspects and Boundary Conditions. *Chem. Mat.* **2018,** *30* , 561-569.

(5) Bard, A. J.; Faulkner, L. R. *Electrochemical Methods: Fundamentals and Applications*. Wiley: New York, USA; 2000.

(6) Serdechnova, M.; Ivanov, V. L.; Domingues, M. R. M.; Evtuguin, D. V.; Ferreira, M. G. S.; Zheludkevich, M. L. Photodegradation of 2-mercaptobenzothiazole and 1,2,3-benzotriazole Corrosion Inhibitors in Aqueous Solutions and Organic Solvents. *Phys. Chem. Chem. Phys.* **2014,** *16* , 25152-25160.

(7) Mashford, B. S.; Stevenson, M.; Popovic, Z.; Hamilton, C.; Zhou, Z.; Breen, C.; Steckel, J.; Bulovic, V.; Bawendi, M.; Coe-Sullivan, S.; Kazlas, P. T. High-Efficiency Quantum-Dot Light-Emitting Devices ith Enhanced Charge Injection. *Nature Photonics* **2013,** *7*, 407.

(8) Giménez, S.; Rogach, A. L.; Lutich, A. A.; Gross, D.; Poeschl, A.; Susha, A. S.; Mora-Seró, I.; Lana-Villarreal, T.; Bisquert, J. Energy Transfer versus Charge Separation in Hybrid Systems of Semiconductor Quantum Dots and Ru-dyes as Potential co-Sensitizers of TiO_2-based Solar Cells. *Journal of Applied Physics* **2011,** *110* , 014314.

(9) Ravi, V. K.; Scheidt, R. A.; Nag, A.; Kuno, M.; Kamat, P. V. To Exchange or Not to Exchange. Suppressing Anion Exchange in Cesium Lead Halide Perovskites with $PbSO_4$–Oleate Capping. *ACS Energy Letters* **2018,** *3* , 1049-1055.